THE JOURNAL OF PHYSICAL CHEMISTRY B

ARTICLE

pubs.acs.org/JPCB

Experimental (IR/Raman and $^{1}H/^{13}C$ NMR) and Theoretical (DFT) Studies of the Preferential Conformations Adopted by L-Lactic Acid Oligomers and Poly(L-lactic acid) Homopolymer

S. Jarmelo,*[,†,‡] D. A. S. Marques,[‡] P. N. Simões,[‡] R. A. Carvalho,[§] C. M. S. G. Batista,[‡] C. Araujo-Andrade,[⊥] M. H. Gil,[‡] and R. Fausto[†]

[†]Department of Chemistry, University of Coimbra, Coimbra 3004-535, Portugal

[‡]Department of Chemical Engineering, University of Coimbra, Coimbra 3030-290, Portugal

[§]Department of Life Sciences and Center for Neurosciences, University of Coimbra, Coimbra 3001-401, Portugal

[⊥]Centro de Investigaciones en Óptica, A. C., Loma del Bosque No. 115, Col. Lomas del Campestre, 37150, León, Guanajuato 37150, Mexico

Supporting Information

ABSTRACT: L-Lactic acid (L-LA) oligomers (up to the pentamer) were studied by three complementary approaches: vibrational (IR and Raman) and NMR (^{1}H and ^{13}C) spectroscopies and DFT calculations. Vibrational and NMR spectra of L-LA oligomers and poly(L-lactic acid) (PLLA) homopolymer were recorded at room temperature and interpreted. Further insight into the structures (conformations) of the title systems was provided by theoretical B3LYP/6-311++G(d,p) studies. Calculated energies and computed vibrational and NMR spectra of the most stable conformers of L-LA oligomers, together with the experimental vibrational and NMR spectra, enabled the characterization of the preferred conformations adopted by PLLA chains.

INTRODUCTION

Poly(L-lactic acid) homopolymer (PLLA), $H-[OCH(CH_3)C{=}O]_n-OH$, is a chiral polyester analogue to poly(L-alanine). PLLA has attracted increasing attention in recent years by virtue of being one of the most promising thermoplastics among the family of environmentally friendly biodegradable polymers.[1] Owing to its good mechanical properties, PLLA has tremendous potential in the traditional applications of thermoplastics.[2] PLLA has also been used as a biocompatible polymer for applications in implant materials, surgical sutures, and controlled drug delivery systems.[3,4]

The mechanical and thermal properties of a crystalline polymer strongly depend on its morphology and crystal structure.[4,5] Additionally, the conformations exhibited by single polymeric chains are crucial for applications as widespread as those evoked above. The investigation of the conformations preferentially adopted by an isolated polymeric chain can also be very useful for the determination of the crystalline structure of polymers, since in many materials the crystalline structure is largely determined by intramolecular interactions.[6] Thus, the study of this type of interactions in the isolated polymer (oligomers) appears to be of interest.

In the present study, a detailed investigation of the energetics and structural and spectroscopic characteristics of small L-LA oligomers and the homopolymer itself was undertaken in order to characterize the preferred conformations adopted by PLLA chains. IR/Raman and $^{1}H/^{13}C$ NMR spectroscopies, known as being very sensitive to structural aspects, were used as the main experimental tools. The interpretation/analysis of experimental spectroscopic data is supported by theoretical calculations. The geometries, energies, and vibrational and $^{1}H/^{13}C$ NMR spectra of L-LA oligomers (up to the pentamer) were studied theoretically at the B3LYP/6-311++G(d,p) level of approximation. In the followed approach, information about the preferred conformations of the PLLA chains was gained step-by-step, starting from investigation of the structure of the monomer and adding other monomers up to the pentamer, used as the model for PLLA homopolymer.

EXPERIMENTAL AND COMPUTATIONAL METHODS

Experimental Section. *Materials.* All materials were ordered from Sigma-Aldrich and used without any additional purification. Monomer, L(+)-lactic acid 80%; solvent, xylene (96%); catalyst, tin(II) chloride dihydrate (98%); molecular sieves, 3 Å beads, 8−12 mesh.

Methods. The synthesis of small L-LA oligomers was done by distillation of the L-LA aqueous solution at 100 °C and atmospheric pressure, under continuous nitrogen flow.

Received: May 30, 2011
Revised: November 11, 2011
Published: November 14, 2011

The PLLA homopolymer was synthesized by the solution polymerization of L-LA, which was carried out using xylene (20% V/V of monomer). The polymerization starts with the distillation of the L-LA aqueous solution in a flask equipped with a Dean−Stark trap. After that, the catalyst (0.1% mol) is introduced and the trap is replaced by a packed tube filled with molecular sieves as a drying agent. The polymerization was performed at the boiling point of the solvent, under inert atmosphere for 30 h. The final product, PLLA homopolymer, was recovered by dissolution in THF and precipitation in methanol.[7]

The great advantage of this method is to make possible a single step synthesis of small oligomers and high molecular weight polymers directly from the L-LA monomer.

Measurements. IR spectra of solid polycrystalline PLLA pressed in a KBr pellet were obtained in the range 4000−600 cm^{-1}, at room temperature, using a Bomem (MB104) Fourier transform spectrometer equipped with a deuterated triglycine sulfide (DTGS) detector and Zn/Se optics. Data collection was performed with 2 cm^{-1} spectral resolution and 128 accumulations.

IR spectra of the oily mixture of small L-LA oligomers were obtained in the range 4000−600 cm^{-1}, at room temperature, using a Magma-IRTM Spectrometer 750 from Nicolet Instrument Corp., equipped with a Golden Gate Single Reflection Diamond ATR. Data collection was performed with 2 cm^{-1} spectral resolution and 128 accumulations.

Raman spectra of solid PLLA and of the oily mixture of small L-LA oligomers were acquired in the range 3380−100 cm^{-1}, at room temperature, using a dispersive Raman instrument, model DXR SmartRaman^{TM} spectrometer from Thermo Fisher Scientific Inc., equipped with a low-power, externally stabilized diode laser, 780 nm excitation wavelength, with a maximum power at output of laser head of 14 mW and a 3.0 mm beam diameter. The PLLA was pressed in a pellet (neat solid), and the data were collected with an exposure time to laser radiation of 100 s, 100 sample exposures, and a slit aperture of 25 μm. No fluorescence correction was applied. The mixture of L-LA oligomers was kept in a glass vial, and the data were collected with an exposure time to laser radiation of 20 s, 10 sample exposures, and a slit aperture of 50 μm. A fifth degree polynomial was applied for fluorescence correction.

^{1}H and ^{13}C NMR spectra of PLLA homopolymer and L-LA oligomers in DMSO-D_6 and $CDCl_3$ solvents, at room temperature, were obtained on a Varian Unity 500 MHz spectrometer using a 5 mm broad-band NMR probe. Samples were prepared by dissolving 10 mg of PLLA or L-LA oligomers in 600 μL of the deuterated solvent. Each proton spectrum consisted of 32 averaged scans, and acquisition parameters included 36k points covering a spectral width of 6 kHz, a 30° radio-frequency excitation pulse, and a total repetition time between scans of 10 s to allow full relaxation. Carbon spectra consisted of 512 averaged scans, and acquisition parameters included 65k points covering a spectral width of 30 kHz, a 45° radio-frequency excitation pulse, and a total repetition time between scans of 3 s to allow full relaxation of aliphatic carbons. Digital zero filling to 64k (proton) and 128k (carbon) and a 0.5 Hz exponential were applied before Fourier transformation. For L-LA oligomers, the DMSO was preferred as solvent, since the NMR analyses of these systems were found considerably improved by recording spectra in DMSO-D_6 instead of $CDCl_3$.[8] Concerning PLLA, due to the low solubility of the homopolymer in DMSO-D_6, only $CDCl_3$ was used as solvent.

The average molecular weight and polydispersity index of PLLA were determined using the SEC (size exclusion chromatography) technique, calibrated with narrow polystyrene standards. The column set consists of a PL 5 μm guard column (50 × 7.5 mm) followed by two MIXED-D PL columns (300 × 7.5 mm, 10 μm). The HPLC pump was set with a flow rate of 1 $mL \cdot min^{-1}$. The eluent was $CHCl_3$, and the experiments were carried out at 25 °C with a sample concentration of ≈2 $mg \cdot mL^{-1}$. Before the injection (≈50 μL), the sample was filtered through a PTFE membrane with a 0.45 μm pore. After column exclusion, the sample was analyzed in an evaporative light scattering detector, PL-EMD 960. The recorded average molecular weight was 3000 $g \cdot mol^{-1}$ and the polydispersity index was 1.5.

Due to the small size of the entities constituting the mixture of the L-LA oligomers, the average molecular weight and polydispersity index were not possible to determine by SEC.

Computational. The first step within the computational framework was a conformational search on the molecular mechanics (MM+ force field) potential energy surface (PES) of the L-LA oligomers (dimer, trimer, and tetramer) to generate a sequence of conformations. A stochastic approach based on modification of selected torsion angles[9] was used, as implemented in the HyperChem program.[10] This first scrutiny enabled the most stable conformers of each L-LA oligomer to be found, whose optimized structures were then used as input geometries for density functional theory (DFT) calculations, performed with the B3LYP functional,[11] using the 6-311++G(d,p) basis set.[12] Geometry optimizations and harmonic frequency calculations were carried out with the Gamess package,[13] whereas the magnetic shielding tensors calculations were performed with the Gaussian03 package[14] using the GIAO (gauge-independent atomic orbital) method [the calculations here presented were performed in vacuo; in this case, the reasonable agreement between experimental (for both DMSO-D_6 and $CDCl_3$ solvents) and calculated results made the use of the considerably more expensive SCRF (self-consistent reaction field) calculations unnecessary].[15] Additional calculations were performed by using two different basis sets specially designed for the prediction of NMR properties: pcS-2[16] and aug-cc-pVTZ-J[17] (see Tables S1−S2; the prefix "S" in the names of figures and tables stands for Supporting Information). It is clear that, for the molecular systems under study, the replacement of the modest 6-311++G(d,p) basis set by the aug-cc-pVTZ-J one leads to a degradation of the predicted ^{13}C chemical shifts, which is even more pronounced when the replacement is made by the pcS-2 basis (very interestingly, a similar trend was recently reported by Kupka[18] in a study focusing on the NMR properties of methanol).

The initial geometry of L-LA pentamer was built from the information earned from the previous studies performed on L-LA smaller oligomers. The procedure here adopted enabled to keep the number of optimization steps for the pentamer very small, and the changes in the structural parameters were also very small. This result indicates that the adopted stepwise strategy, starting from monomer and increasing subsequently the size of the oligomers, has good predictive capabilities.

For the L-LA monomer, systematic conformational searches on the molecular mechanics (MM+ force field)[10] and semiempirical (PM3[19] and PM6[20]) PES were undertaken in order to test the abilities of these less demanding computational methods in predicting structural, energetic, and spectroscopic properties of the systems under study. The molecular mechanics calculations

were performed with the HyperChem program,[10] and the semiempirical calculations with MOPAC2007.[21]

RESULTS AND DISCUSSION

The ultimate objective of this work is the determination of the most probable conformations adopted by L-LA homopolymer chains. To achieve this goal, the L-LA monomer and small L-LA oligomers (up to the pentamer) were studied. In order to conclude about the relative performance of the different types of calculations tested in this study, the corresponding results were compared with experimental vibrational and NMR data.

The results obtained for L-LA monomer are presented and discussed separately, since this species was used essentially to find the appropriate level of theory to be used in the prediction of energetic, structural, and vibrational properties of L-LA oligomers. On the other hand, the results obtained for L-LA dimer, trimer, and tetramer are presented and discussed all together. The main objective of the study of these small oligomers was to determine their conformational preferences and to transfer the gained information to larger L-LA oligomers. In particular, specific relative spatial arrangements of groups around specific bonds will be considered in detail. Finally, the L-LA pentamer, which was found to be the smallest oligomer that can mimic the general homopolymer properties, will be analyzed jointly with PLLA.

L-Lactic Acid Monomer. *Geometries and Energies.* L-LA monomer has three internal rotation axes that can give rise to conformational isomers (O_A-C, $C-C$, $C-O_C$; in reference to the OH groups, the subscript A stands for alcohol and the subscript C stands for carboxylic throughout this article). Table 1 shows the values of the $H_A-O-C-C$, $O_A-C-C=O$, and $O=C-O-H_C$ dihedral angles for L-LA conformers calculated at the different levels of theory used in this study (MM, PM3, and PM6, and DFT). The conformers are depicted in Figure 1. Full structural and energetic data are provided in Table S3.

The conformers are denoted by names formed according to the following systematic rules: the first letter refers to the $H_A-O-C-C$ torsion angle (S = *syn*, torsion angle between −30° and 30°; A = *anti*, torsion angle between 150° and −150°; G = *gauche*, torsion angle between 30° and 90°; G′ = *gauche′*, torsion angle between −30° and −90°); the second letter refers to the $O_A-C-C=O$ torsion angle (S; A; G; G′; SK = *skew*, torsion angle between 90° and 150°; SK′ = *skew′*, torsion angle between −90° and −150°), and the third letter refers to the $O=C-O-H_C$ torsion angle (C = *s-cis*, ≈ 0°; T = *s-trans*, ≈ 180°).

From a chemical point of view, L-LA belongs to the family of α-hydroxy acids, whose simplest member is glycolic acid ($HO-CH_2-COOH$). This is by far the most studied member of the family, both experimentally and theoretically.[22] The available studies on glycolic acid indicate that the most stable conformer is the intramolecularly H-bonded form SSC, with a planar heavy-atom skeleton and a five-member ring closed by the intramolecular H-bond. The analogous dimethyl-substituted derivative of glycolic acid, α-hydroxy isobutyric acid [$HO-C(CH_3)_2-COOH$], has also been previously studied, both experimentally and theoretically.[23] The SSC conformer was also found to be the preferred form of this molecule.

Whatever the theoretical method used in this investigation, the predicted most stable form of monomeric L-LA exhibits an H-bond between the α-hydroxyl group and the carbonyl oxygen atom, like the conformational ground state of both glycolic and α-hydroxy isobutyric acids (Table 1; Figure 1). However, at MM and semiempirical PM3 and PM6 levels of theory, both $H_A-O-C-C$ and $O_A-C-C=O$ dihedrals are substantially deviated from the plane containing the carboxyl group. This tendency is observed for almost all conformers (Tables 1 and S3). Contrarily to the MM and semiempirical calculations, the DFT method predicts considerably more planar $H_A-O-C-C$ and $O_A-C-C=O$ fragments in most of the conformers (**I-M**, **IV-M**, **V-M**, **VI-M**, and **VII-M**; Table 1). Furthermore, while the MM and semiempirical calculations predict a set of conformers where the $O_A-C-C=O$ dihedral assumes the G′ conformation, such structures are not predicted to be minimum energy conformations at the DFT level. For example, in conformers **I-M**, **V-M**, and **VII-M** optimized at the DFT level of theory, the $O_A-C-C=O$ dihedral adopts a *syn*

Table 1. Most Relevant Dihedrals (deg) of L-Lactic Acid Monomer Calculated at Molecular Mechanics (MM+ Force Field), Semiempirical PM3 and PM6, and B3LYP/6-311++G(d,p) Levels of Theory[a]

conformers[b]	MM[c]	PM3	PM6	B3LYP[e]
I-M	G′G′C	GG′C[d]	GG′C[d]	SSC
$H_A-O-C-C$	−63.8	61.1	61.2	0.3
$O_A-C-C=O$	−43.8	−39.0	−41.2	−3.0
$O=C-O-H_C$	−1.9	2.3	1.3	−0.2
II-M	GSKC	GSKC	GSKC	GSKC
$H_A-O-C-C$	63.4	67.6	59.4	51.5
$O_A-C-C=O$	121.5	146.6	148.8	149.9
$O=C-O-H_C$	0.5	−1.8	−2.6	−0.4
III-M	G′SKC	G′AC	G′AC	G′AC
$H_A-O-C-C$	−64.0	−59.8	−47.8	−43.3
$O_A-C-C=O$	132.6	−157.6	−155.9	−156.8
$O=C-O-H_C$	1.9	2.5	3.2	0.3
IV-M	ASKT	GAT	GAT	AAT
$H_A-O-C-C$	−173.9	81.6	98.4	162.2
$O_A-C-C=O$	133.9	−159.3	−171.3	174.1
$O=C-O-H_C$	−179.7	−177.3	−177.0	−179.3
V-M	AG′C	GG′C[d]	GG′C[d]	ASC
$H_A-O-C-C$	−174.1	62.6	60.6	172.7
$O_A-C-C=O$	−40.7	−44.1	−40.6	−18.2
$O=C-O-H_C$	−1.5	0.5	−0.5	−1.1
VI-M	ASKC	ASKC[f]	GSKC	AAC
$H_A-O-C-C$	−174.1	153.4	60.1	172.8
$O_A-C-C=O$	132.5	122.9	142.3	153.2
$O=C-O-H_C$	1.4	−3.0	−1.7	−1.0
VII-M	G′G′T	GG′T	GG′T	SST
$H_A-O-C-C$	−64.3	57.2	53.8	1.6
$O_A-C-C=O$	−36.9	−33.8	−28.8	−3.9
$O=C-O-H_C$	179.9	178.4	177.7	179.9

[a] The subscript A stands for alcohol, while the subscript C stands for carboxylic group. S, *syn* ≈ 0°; G/G′, *gauche/gauche′* ≈ 60/−60°; SK/SK′, *skew/skew′* ≈ 120/−120°; A, *anti* ≈ 180°; C, *s-cis* ≈ 0°; T, *s-trans* ≈ 180°. [b] Conformers of L-lactic acid monomer calculated at B3LYP/6-311++G(d,p) level of theory are depicted in Figure 1. [c] Vibrational spectra were not calculated. [d] Conformer **V-M** converged into conformer **I-M** at both semiempirical PM3 and PM6 levels of theory. [e] From Borba, A.; Gómez-Zavaglia, A.; Lapinski, L.; Fausto, R. *Phys. Chem. Chem. Phys.* **2004**, *6*, 2101. [f] First order transition state.

dx.doi.org/10.1021/jp205033c | *J. Phys. Chem. B* 2012, 116, 9–21

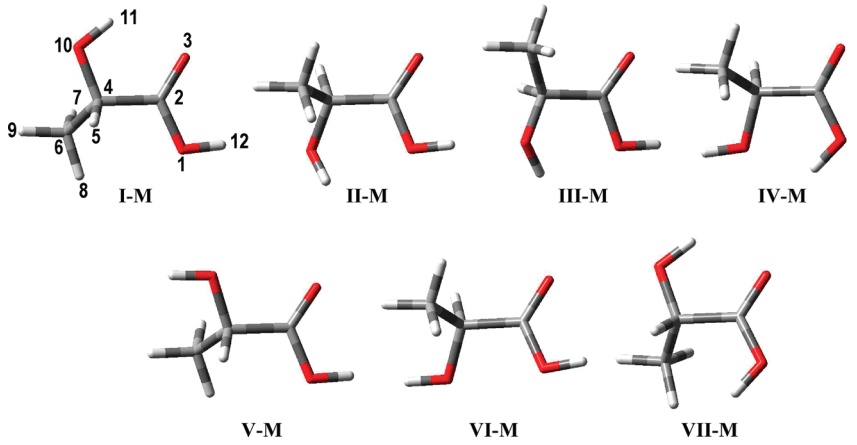

Figure 1. Conformers of L-LA monomer calculated at the B3LYP/6-311++G(d,p) level of theory (Borba, A.; Gómez-Zavaglia, A.; Lapinski, L.; Fausto, R. *Phys. Chem. Chem. Phys.* **2004**, *6*, 2101).

conformation, while the MM and semiempirical methods yield this dihedral in a G′ orientation. The DFT calculations performed on glycolic and α-hydroxy isobutyric acids also do not predict any minimum energy conformation bearing the $O_A-C-C=O$ dihedral in a G/G′ arrangement.[22,23] Thus, with respect to conformational analysis, not very encouraging results were obtained for L-LA monomer using the MM and semiempirical PM3 and PM6 methods.

Vibrational Spectra. L-LA has 30 fundamental vibrations, all active in IR and Raman. Table S4 displays the calculated spectra and approximate description of the normal modes for the most stable conformer, **I-M**, which is expected to be the experimentally most relevant one (Boltzmann's population at 300 K: MM, 100.0%; PM3, 73.3%; PM6, 46.9%; B3LYP, 91.5%). In order to conclude on the quality of the vibrational calculations performed at the different levels of approximation used, the experimental IR spectrum of L-LA monomer isolated in an Ar matrix[24] is also presented in this table.

Concerning the calculation of the IR spectrum of L-LA monomer at the semiempirical PM3 level of theory, the available appropriate factors to correct the frequencies[25] reproduce in general reasonably well the experimental results. Unfortunately, the correction factors for the modes involving oxygen atoms are not available. On the other hand, there are several works where a single scaling factor for PM3 and PM6 vibrational frequencies was proposed, but this type of correction is not, in fact, appropriate for this type of calculations,[26] where the deviations of calculated frequencies from experimental values are far from being systematic and, then, uniformly scalable. Based on the good agreement with the experimental results, the B3LYP/6-311++G(d,p) calculations were here selected for the study of the larger L-LA oligomers.

NMR Spectra. Table S5 shows the calculated chemical shifts (^{1}H, ^{13}C, and ^{15}O) for the conformers of L-LA monomer shown in Figure 1 and the experimental chemical shifts (^{1}H and ^{13}C) with respect to TMS. The agreement between calculated [GIAO B3LYP/6-311++G(d,p)] and experimental data is reasonable, justifying the use of this level of theory in the prediction of the chemical shifts of the investigated larger L-LA oligomers. Results obtained with the pcS-2 and aug-cc-pVTZ-J basis sets were found to deviate more from the experimental data than that obtained using the 6-311++G(d,p) basis set.

L-Lactic Acid Dimer, Trimer, and Tetramer. The L-LA dimer, trimer, and tetramer allow the investigation of properties dependent on internal axes of rotation that are absent in L-LA monomer but are present in the PLLA homopolymer chains: $C-O_E$ and O_E-C (throughout this article, the subscript E stands for ester).

Based on the evaluation of the relative performance of the various theoretical methods used to investigate the L-LA monomer described above, the structural, energetic, and spectroscopic properties of the higher L-LA oligomers were studied at the B3LYP/6-311++G(d,p) level of approximation. However, due to the large number of possible conformers that L-LA oligomers can exhibit, a preliminary conformational search performed using molecular mechanics was undertaken to select a range of putative low energy geometries, later on utilized as starting structures for the higher level B3LYP/6-311++G(d,p) calculations.

Geometries and Energies. The geometric parameters of the intramolecular H-bonds that stabilize the conformers of monomeric L-LA and respective oligomers here investigated, dimer, trimer, and tetramer, are presented in Table S6.

Dimer. From the conformational search performed on the MM PES of L-LA dimer, 37 different structures were located with relative energies up to 25 kJ mol^{-1} (Table S7). The eight most stable geometries optimized at this level of theory, with energies up to ca. 10 kJ mol^{-1}, were then used as starting geometries for the B3LYP/6-311++G(d,p) calculations. At this level of theory, only five conformers were obtained within a range of relative energy of ca. 35 kJ mol^{-1} (conformers are depicted in Figure S1 and structural parameters and relative energies are shown in Table S8).

As could be anticipated, the calculations predict the most stable form of dimeric L-LA, **I-D**, bearing an H-bond between the α-hydroxyl group and the neighbor carbonyl oxygen atom of the ester group of the alcohol unit [$CH_3CH(OH)-C(=O)O-$; Figure S1] and having the carboxylic group in a *s-cis* orientation. These trends are analogous to those obtained for the conformational ground state of the monomer. On the other hand, the *gauche*′ conformation of the $C-O_E-C-C$ dihedral was found to be the preferred arrangement of this fragment, being observed in the two most stable dimers (**I-D** and **II-D**) and also in **IV-D**.

From the calculations performed on the dimer, one can thus conclude that the $O-H_A\cdots O=$ intramolecular H-bond (**I-D** and **III-D**), the *s-cis* conformation of the $O=C-O-H_C$ dihedral (found in all the five lowest energy conformers), and the *gauche*′ conformation of the $C-O_E-C-C$ dihedral (**I-D**, **II-D**, and **IV-D**)

dx.doi.org/10.1021/jp205033c |*J. Phys. Chem. B* 2012, 116, 9–21

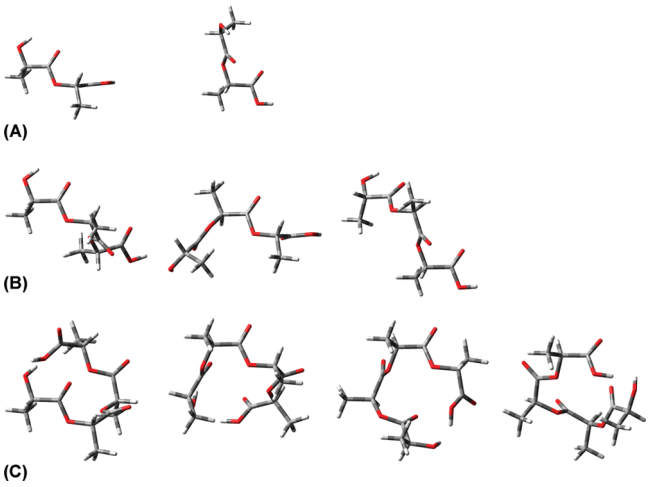

Figure 2. Different views of the most stable conformation (global minimum) of L-LA dimer (A), trimer (B), and tetramer (C) found at the B3LYP/6-311++G(d,p) level of theory.

play a very important role in the stabilization of the molecule. It can be assumed that these stabilization energetic factors apply for the dimeric unit within the polymeric PLLA chain as well. Moreover, the *syn* arrangement of the ester group ($O{=}C{-}O_E{-}C \approx 0°$) was also observed for all low energy conformers of the dimer investigated. This observation is in agreement with the general conclusions from microwave and IR spectroscopies and electron diffraction on the preferred conformations of carboxylic esters.[27]

Trimer. During the conformational search performed on the MM PES of the L-LA trimer, 470 different structures with energies up to 25 kJ mol^{-1} were located (Table S9). The 20 most stable of these structures, with relative energies up to 3 kJ mol^{-1}, were used as starting geometries for the B3LYP/6-311++G(d,p) calculations. [Instead of an energy cutoff of 10 kJ mol^{-1}, as used for the dimer, a tight one of just 3 kJ mol^{-1} was used for the trimer, reducing the number of conformations from ca. 170 to 20 (Table S9)]. At this level of theory, 18 conformers were obtained, within a range of energy of ca. 27 kJ mol^{-1}. Table S10 shows the relevant structural parameters and relative energies for the L-LA trimers, whose conformers are depicted in Figure S2.

Similarly to the results obtained for the dimer, the B3LYP calculations predict the most stable form of L-LA trimer, **I-Tri**, with an H-bond from the hydroxyl alcohol group to the neighbor carbonyl oxygen atom of the ester group (Figure S2), the carboxylic group in the *s-cis* orientation, and a *syn* conformation around the $C{-}O_E$ bonds. The *syn* conformation around the $C{-}O_E$ bond is indeed observed in all low energy conformers of the L-LA trimer. All studied low energy conformers also adopt the same conformation about the $O_E{-}C_{12}{-}C_{13}{=}O$ dihedral: *anti* (see Figure S2 for atom labeling).

Conformers **I-Tri** and **XV-Tri** only differ in the orientation of the $H_A{-}O{-}C{-}C$ dihedral, *syn* and *anti*, respectively. **XV-Tri** is higher in energy than **I-Tri** by ca. 20 kJ mol^{-1}. The fact that in **XV-Tri** the orientation exhibited by the alcohol group does not allow the establishment of any intramolecular H-bond justifies the relative energies of these two conformers.

On the other hand, conformers **II-Tri** and **VIII-Tri** differ only in the orientation of the $O_E{-}C_{21}{-}C_{23}{=}O_C$ dihedral, *syn* and *anti*, respectively. Rotating the $C_{21}{-}C_{23}$ single bond of conformer **II-Tri** by 180° to obtain conformer **VIII-Tri** raises the energy of the molecule by ca. 8 kJ mol^{-1}. In both conformers the $O{-}H_A$ group acts as proton donor, but due to the different orientations around the $O_E{-}C_{21}{-}C_{23}{=}O_C$ dihedral, the proton acceptors are different ($O_{Carbonyl}$ in conformer **II-Tri** and $O_{Carboxyl}$ in **VIII-Tri**). The carbonyl oxygen is a better proton acceptor,[28] thus justifying the relative energies of these two conformers.

Conformers **II-Tri** and **XVIII-Tri** [$\Delta E_{(\text{II-Tri}-\text{XVIII-Tri})}$ = 26.9 kJ mol^{-1}] only differ in the orientation of $O{=}C{-}O{-}H_C$ dihedral, which is *s-cis* and *s-trans*, respectively. In general, the *s-cis* arrangement of the $O{=}C{-}O{-}X$ group is more stable than the *s-trans*.[29] This general trend has been explained considering (i) steric and electrostatic repulsions between −X and −R groups (R−COOX; X = H—carboxylic acid and X = alquil or benzyl—carboxylic ester), (ii) bond dipolar interactions associated with C=O and O−X bonds, and (iii) mesomerism.[30] Conformer **V-Tri** is the most stable among those in which the carboxylic group adopts the much less stable *s-trans* conformation. The position of this conformer in terms of relative stability is explained by the three intramolecular H-bonds, $O{-}H_A{\cdots}O{=}$, $O{-}H_C{\cdots}O{=}$, and $O{-}H_C{\cdots}O_E$ (Table S6), that it can establish. The intramolecular H-bonds in which the $O{-}H_C$ group is involved as proton donor are just possible due to the *s-trans* orientation of the carboxylic moiety.

The six most stable conformers of L-LA trimer, whose relative energies fall within a ca. 3 kJ mol^{-1} interval (Table S10), exhibit an $O{-}H_A{\cdots}O{=}$ intramolecular H-bond. This is the most relevant stabilizing interaction in these L-LA oligomers. Other less important interactions can stabilize the L-LA trimer, such as weaker intramolecular H-bonds of type $O{-}H_A{\cdots}O_C$, $O{-}H_A{\cdots}O_E$, $O{-}H_C{\cdots}O{=}$, $O{-}H_C{\cdots}O_A$, and $O{-}H_C{\cdots}O_E$ (Table S6).

Tetramer. During the conformational search performed on the MM PES of the tetramer, 463 different structures with energies up to 25 kJ mol^{-1} were located (Table S11). The most stable geometries optimized at the MM level of theory, with energies up to 3 kJ mol^{-1} (11 conformers), were then used as starting structures for the B3LYP/6-311++G(d,p) calculations. At the higher level of theory, also 11 conformers (see Figure S3) within a range of energy of ca. 45 kJ mol^{-1} were obtained. Table S12 shows the structural parameters and relative energies of the most stable forms of the L-LA tetramer calculated at the B3LYP/6-311++G(d,p) level of theory.

All tetramer conformers adopt the *syn* conformation for the three $O{=}C{-}O_E{-}C$ dihedrals ($O{=}C_1{-}O_{15}{-}C_{12}$/ $O{=}C_{13}{-}O_{E1}{-}C_{21}$/$O{=}C_{23}{-}O_{E2}{-}C_{31}$). Moreover, for all conformers, the $O_{15}{-}C_{12}{-}C_{13}{=}O$ dihedral is *anti* and the $C_1{-}O_{15}{-}C_{12}{-}C_{13}$ dihedral is *gauche'*. The *syn* orientation around the $C{-}O_E$ bond is also adopted by all dimers and trimers investigated (Tables S8 and S10), and the *anti* conformation of the $O_{15}{-}C_{12}{-}C_{13}{=}O$ dihedral by the equivalent dihedral in all low energy trimers (Table S10).

The four most stable conformers of L-LA tetramer have an $O{-}H_A{\cdots}O{=}$ intramolecular H-bond ($\Delta E_{\text{IV-Tetra}-\text{I-Tetra}} \approx 3$ kJ mol^{-1}; Tables S6 and S12). As observed for the smaller oligomers, this is the most relevant stabilizing interaction in these systems. As expected, B3LYP/6-311++G(d,p) calculations predict the most stable form of L-LA tetramer, **I-Tetra**, bearing an intramolecular H-bond between the hydroxyl group of alcohol and the neighbor carbonyl oxygen atom, forming a

dx.doi.org/10.1021/jp205033c |*J. Phys. Chem. B* 2012, 116, 9–21

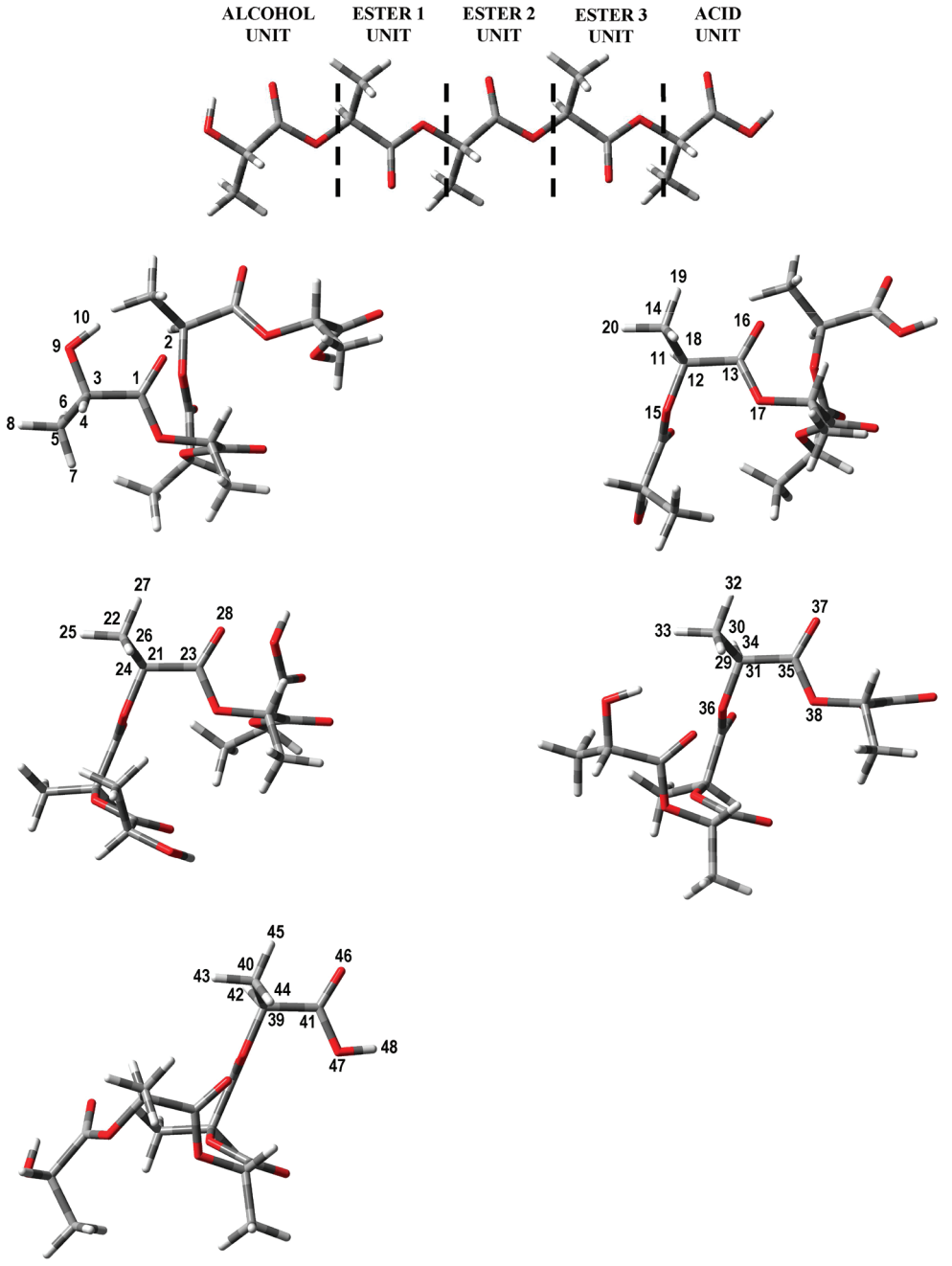

Figure 3. Different views of the conformer SS[SG′A]$_4$C of L-LA pentamer calculated at the B3LYP/6-311++G(d,p) level of theory. The atom numbering and the labeling of the five monomeric units that constitute the oligomer are presented.

five-membered ring (Figure S3). Other less important interactions can stabilize the L-LA tetramer, such as O−H$_A$···O$_E$, O−H$_C$···O=, O−H$_C$···O$_A$, and O−H$_C$···O$_E$ (Table S6). The latter intramolecular H-bond interactions are contributing to the stabilization of the seven most stable conformers ($\Delta E_{\text{VII-Tetra}-\text{I-Tetra}} \approx 17$ kJ mol^{-1}; Tables S6 and S12). The remaining studied conformers, i.e., **VIII-Tetra**−**XI-Tetra**, do not establish any intramolecular H-bond, lying in a relative energy range of 17−45 kJ mol^{-1} (Tables S6 and S12).

In summary, as observed for the monomer, dimer, and trimer, the O−H$_A$···O═ intramolecular H-bond and the *s-cis* conformation of the O═C−O−H$_C$ dihedral play important roles in the stabilization of the tetramer conformers. [The position of the O−H$_A$ stretching vibration, in which the hydroxyl group is experiencing different environments, is an adequate parameter to account for the strength of the most relevant interaction that stabilizes the L-LA oligomers, O−H$_A$···O═ (both groups, hydroxyl and carbonyl, are located in the alcohol unit, see Figure 3 below for units labeling): the B3LYP/6-311++G(d,p) calculations predict a red shift of ca. 100 cm^{-1} going from the free O−H$_A$ group to the group involved in an H-bond with the neighbor carbonyl group (see Table S6)]. The intramolecular H-bond established between the O−H$_A$ and the neighbor carbonyl oxygen atom forces the H$_A$−O−C−C and O$_A$−C−C═O dihedrals to adopt a *syn* conformation. Thus, one can say that the study on the monomer itself allows to conclude on the conformation adopted

dx.doi.org/10.1021/jp205033c |*J. Phys. Chem. B* 2012, 116, 9–21

Scheme 1. Most Stable Conformations Adopted by the Independent Dihedrals of a PLLA Homopolymer Constituted by *n* L-LA Monomers [SS(SG′A)$_{n-1}$C]

$$H_A\text{–}\left[O\text{–}C\text{–}C(=O)\text{–}O_E\text{–}C\text{–}C(=O)\right]_{n-1}\text{–}O\text{–}H_C$$

Dihedral	Conformation	Information obtained:
H_A–O–C–C	*syn* (S)	MONOMER
O–C–C(=O)	*syn* (S)	MONOMER
O=C–O_E–C	*syn* (S)	DIMER
C–O_E–C–C	*gauche'* (G')	TETRAMER
O_E–C–C=O	*anti* (A)	TRIMER
C(=O)–O–H_C	*s-cis* (C)	MONOMER

by the terminal groups of the polymer [SS–(*conformation of polymeric chain)*–C]. The calculations performed on the most stable conformers of the L-LA dimer lead to the conclusion that the preferred conformation adopted by the O=C–O_E–C dihedrals is *syn*. The most stable conformers of L-LA trimer present an *anti* preference for the O_E–C–C=O dihedrals. Finally, the study performed on the most stable conformers of L-LA tetramer confirms the preferred conformation adopted by the C–O_E–C–C as being the *gauche′* one. Scheme 1 summarizes the conclusions reached stepwise in this study regarding the conformational preferences of the studied systems.

Figure 2 shows different views of the most stable conformer of L-LA dimer, trimer , and tetramer.

Vibrational and NMR Spectra. Although it is not possible to assign features due to a specific oligomer in the experimental vibrational (IR and Raman) spectra of the obtained mixture of L-LA oligomers, the calculation of the vibrational spectra for the most stable conformations of each L-LA oligomer was performed, to ensure that the obtained structures are true minima and, consequently, other properties, such as chemical shifts, could be calculated on these structures. Tables S13, S14, and S15 show the calculated and experimental chemical shifts (^{1}H and ^{13}C) with respect to TMS for the structures of L-LA dimer, trimer, and tetramer, respectively. The agreement between calculated and experimental data for all of these oligomers can be considered as being reasonable, validating the use of this type of calculations in the prediction of the spectra of larger L-LA-based systems.

L-Lactic Acid Pentamer and PLLA Homopolymer. Taking into account the structural results for smaller L-LA oligomers, the preferential conformation of the L-LA pentamer, and of higher oligomers and homopolymer itself, was established, and the vibrational and NMR data calculated for the pentamer were used in the interpretation of the experimental data (IR, Raman, and ^{1}H and ^{13}C NMR spectra) obtained for the PLLA homopolymer.

Based on the findings shown in Scheme 1, it can be concluded that (i) the preferred conformation adopted by the L-LA pentamer has an intramolecular H-bond established between the O–H_A group and the neighbor carbonyl oxygen atom, forcing the H_A–O–C–C and O_A–C–C=O dihedrals to adopt a *syn* conformation; (ii) the O=C–O_E–C, C–O_E–C–C, and O_E–C–C=O dihedrals adopt the *syn*, *gauche′*, and *anti* conformations, respectively; (iii) the O=C–O–H_C dihedral has a *s-cis* conformation. Thus, using the same notation as presented before, the most stable conformation of the L-LA pentamer is SSSG′ASG′ASG′ASG′AC, or SS[SG′A]$_4$C (Figure 3). Consequently, the conformation adopted by the polymeric chains of PLLA constituted by *n* L-LA monomers can be written as SS[SG′A]$_{n-1}$C.

Table 2. Structural Parameters of the Most Stable Conformation of L-LA Pentamer Calculated at the B3LYP/6-311++G(d,p) Level of Theory

dihedrals (deg)	SS[SG′A]$_4$C
H–O_A–C–C[a]	−8.2
O_A–C–C=O	1.2
O_A=C–O_A–C	−1.8
C–O_A–C–C	−86.8
O_A–C–C=O_{E1}	174.7
O_{E1}=C–O_{E1}–C	−2.4
C–O_{E1}–C–C	−92.2
O_{E1}–C–C=O_{E2}	−178.4
O_{E2}=C–O_{E2}–C	−4.7
C–O_{E2}–C–C	−86.4
O_{E2}–C–C=O_{E3}	176.7
O_{E3}=C–O_{E3}–C	−1.0
C–O_{E3}–C–C	−78.9
O_{E3}–C–C=O_C	171.7
O_C=C–O_C–H	−2.1

[a] The oxygen atoms are labeled in terms of pentamer's monomeric units (Figure 3).

Table 2 shows the B3LYP/6-311++G(d,p) optimized structural parameters of the SS[SG′A]$_4$C conformation of the L-LA pentamer.

Vibrational Spectra. The L-LA pentamer, used as model in the interpretation of the experimental vibrational (IR and Raman) spectra of PLLA homopolymer, has 138 fundamental vibrations, all active in the IR and Raman spectra. Table S16 displays the B3LYP/6-311++G(d,p) calculated IR and Raman spectra and approximate description of the normal modes for the SS[SG′A]$_4$C conformer of L-LA pentamer. Table 3 shows the experimental spectra of PLLA and of a mixture of small L-LA oligomers. The B3LYP/6-311++G(d,p) calculated vibrational frequencies for the pentamer of L-LA, used to support the assignment of the vibrational experimental spectra, are also presented.

Figures 4 and 5 depict the experimental IR and Raman spectra, respectively, of the mixture of small L-LA oligomers and of the PLLA homopolymer. The B3LYP/6-311++G(d,p) calculated data are also presented in these figures.

As can be seen from Figures 4 and 5 and Table 3, the IR and Raman spectra of the mixture of small L-LA oligomers and of the PLLA homopolymer are very similar. As expected, the similarity clearly increases with the increase of the chain length of the oligomers. There is a good agreement between the experimental and calculated spectra.

As expected, the –OH (alcohol and acid) groups, only present as terminal fragments of PLLA homopolymer (and L-LA oligomers), give rise to a very weak and broad IR bands, which are difficult to distinguish from the background. Additionally, the shape of the IR bands due to residual water present in the samples does not allow observation of the OH features. Thus, for these systems, mixture of L-LA oligomers and PLLA homopolymer, the OH stretching vibration is not a suitable probe for the investigation

dx.doi.org/10.1021/jp205033c |*J. Phys. Chem. B* 2012, 116, 9–21

Table 3. Experimental Vibrational (IR and Raman) Spectra of the PLLA Homopolymer and of the Mixture of Small L-LA Oligomers and Calculated B3LYP/6-311++G(d,p) Vibrational Spectra of the L-LA Pentamer [SS[SG′A]$_4$C][a]

	experimental				
	IR		Raman		
approximate descripton	PLLA	L-LA olig	PLLA	L-LA olig	calcd
νOH_C	3646 (vw)[b]; 3525 (vw)[b]	n.o.[c]	n.i.[d]	n.i.	3675
νOH_A		n.o.	n.i.	n.i.	3665
νCH_3 as	3000 (w)	2990 (w)	2998 (s)	2997 (s)	3065−3045
νCH; νCH_3 s	2952 (w); 2885 (sh)	2943 (w); 2915 (sh)	2945 (vs); 2900 (sh)	2945 (vs); 2886 (sh)	3025−2925
$\nu C{=}O$	1749 (vs)	1735 (vs)	1762 (m)	1749 (m)	1770−1735
δCH_3 as	1453 (m)	1456 (m)	1452 (s)	1454 (s)	1470−1460
δCH_3 s; δCH	1376 (sh); 1362 (m); 1299 (vw); 1262 (vw)	1378 (w); 1268 (vw)	1385 (m); 1365 (sh); 1292 (m)	1386 (w); 1299 (m)	1385−1260
γCH	1205 (sh); 1179 (s)	1214 (s,b)	1215 (m); 1180 (m)	1205 (b)	1245−1210
γCH_3	1128 (s); 1085 (vs)	1128 (s); 1099 (m)	1129 (m); 1091 (m)	1132 (m);1089 (m)	1135−1070
νC_α-C_β	1043 (s)	1046 (m)	1042 (m)	1045 (m)	1045−1005
$\nu O_{Ester}{-}C_\alpha$; $\nu C{-}C_\alpha$	958 (vw); 922 (w); 871 (m); 825 (sh)	922 (w); 900 (sh); 871 (w); 823 (w)	970 (vb); 920 (w); 872 (s)	921 (w); 901 (w); 871 (s); 825 (s)	940−800
$\gamma C{=}O$	750 (w); 691 (m); 670 (sh)	754 (vw)	735 (w); 707 (w); 678 (sh)	741 (m)	755−730
$\tau C{-}O_E$; $\delta O = CO_E$; $\delta CC{=}O$; γCCC[e]	n.i.	n.i.	596 (w); 510 (w); 408 (m); 394 (m); 340 (sh); 305 (m); 249 (w); 237 (w)	645 (w); 562 (sh); 535 (w); 463 (vw); 412 (sh); 390 (m); 341 (w); 305 (sh); 243 (w)	640−245
τC_α-C_β			212 (w); 156 (m)	221 (sh)	230−25

[a] Vibrational frequencies are in cm^{-1}. Qualitative experimental intensities are given in brackets (vw, very weak; w, weak; m, medium; s, strong; vs, very strong; sh, shoulder; b, broad). See Table S16 for the assignment of the calculated IR and Raman spectra of the conformer SS[SG′A]$_4$C of L-LA pentamer. [b] The intensity of these two features is weak, being difficult to assign it to a νOH vibration. The former vibration appears at lower wavenumbers in the IR spectra of L-lactic acid in the crystal (3431 cm^{-1}) (Borba, A.; Gómez-Zavaglia, A.; Lapinski, L.; Fausto, R. *Phys. Chem. Chem. Phys.* **2004**, *6*, 2101), indicating that the hydroxyl group is involved in stronger H-bonds in the crystal than in the polymer. [c] n.o.: not observed. [d] n.i.: not investigated. [e] This set of vibrational modes are not sorted in a narrow and specific wavenumbers spectral region, but, instead, they appear randomly in a quite wide spectral region, i.e., 640−245 cm^{-1}.

dx.doi.org/10.1021/jp205033c | *J. Phys. Chem. B* 2012, 116, 9−21

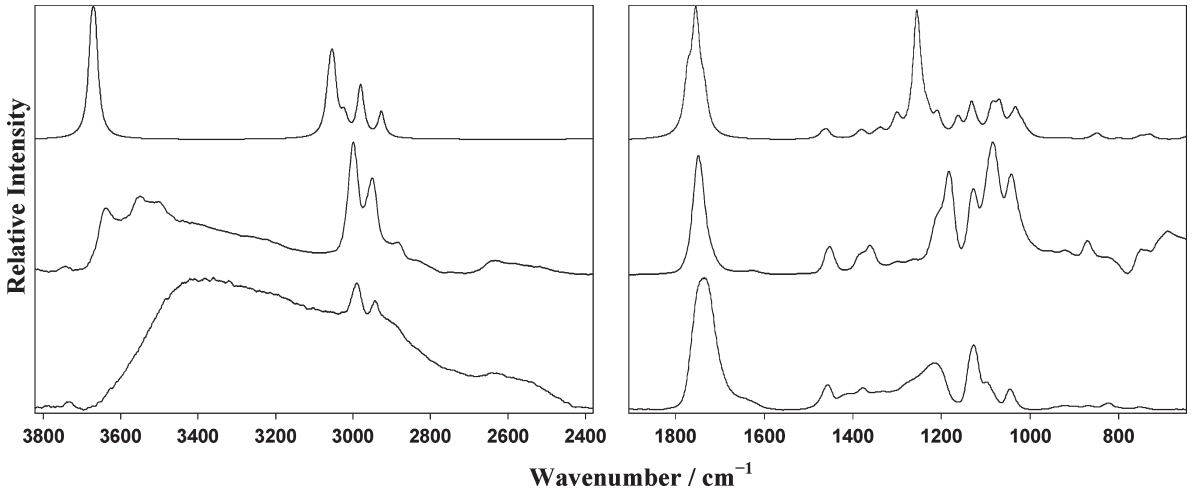

Figure 4. IR spectra in a 3800−650 cm^{-1} spectral region. Bottom: experimental ATR spectrum of an oily mixture of small L-LA oligomers recorded at room temperature. Middle: experimental absorption spectrum of solid PLLA diluted in a KBr pellet recorded at room temperature. Top: B3LYP/6-311++G(d,p) simulated spectrum of L-LA pentamer in vacuo. The calculated wavenumbers were scaled by a factor of 0.978. For the simulation, Lorentzian functions centered at the scaled calculated wavenumbers and with bandwidths at half-height equal to 20 cm^{-1} were used. In order to remove the water of the PLLA homopolymer and a mixture of small L-LA oligomers samples, they were kept in a vacuum oven for several days. However, the water removal process was not 100% efficient, since the bands of water (stretching and bending regions) are present in the IR spectra, mainly in that of the mixture of small L-LA oligomers. It was observed for several samples of polymers and oligomers that it is much more difficult to remove the water from an oily mixture of small oligomers than that of the solid homopolymer.

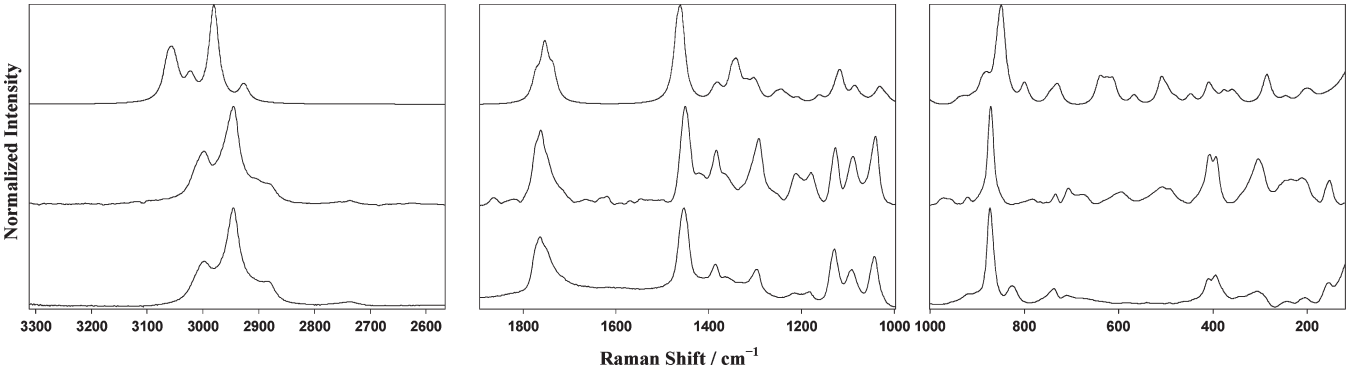

Figure 5. Raman spectra in a 3300−150 cm^{-1} spectral region. Bottom: experimental spectrum of an oily mixture of small L-LA oligomers recorded at room temperature. Middle: experimental spectrum of solid PLLA polymer recorded at room temperature. Top: B3LYP/6-311++G(d,p) simulated spectrum of L-LA pentamer in vacuo. The calculated wavenumbers were scaled by a factor of 0.978. For the simulation, Lorentzian functions centered at the scaled calculated wavenumbers and with bandwidths at half-height equal to 20 cm^{-1} were used.

of any type of intra/intermolecular interaction (see Table 3 for a tentative assignment of the bands due to $\nu OH_{A/C}$ vibrations).

The IR and Raman spectra of L-LA oligomers and PLLA homopolymer in the range of 3100−2885 cm^{-1} show the bands due to the alkyl groups, i.e., −CH and $-CH_3$, characteristic of L-LA oligomers and polymer. These bands are weak in the IR and strong in the Raman spectra.

The C═O stretching vibrations give rise to strong bands in the IR spectra and bands with medium intensity in the Raman spectra. They are observed in the 1762−1735 cm^{-1} range and predicted in the 1770−1735 cm^{-1} range. The assignment of these bands agrees with the assignment made by Blazewicz et al.[31]

The band at ca. 1455 cm^{-1} in the IR (medium intensity) and Raman (strong intensity) spectra of L-LA oligomers and PLLA homopolymer is assigned to the asymmetric bending vibrations of methyl groups (δCH_3 as). The bands due to the symmetric bending vibrations of methyl groups (δCH_3 s) and those due to the bending vibrations of methine groups (δCH) are predicted to appear at lower wavenumbers (1385−1260 cm^{-1} range). Thus, accordingly, the bands in the IR and Raman spectra of L-LA oligomers and PLLA homopolymer that appear in this spectral region are assigned to δCH_3 s and δCH modes.

The out-of-plane bending of methine groups (γCH) appears as a doublet in both the IR (1205 and 1179 cm^{-1}; strong intensity) and Raman (1215 and 1180 cm^{-1}; medium intensity) spectra of the PLLA homopolymer and as a single broad band in the IR (1214 cm^{-1}) and Raman (1206 cm^{-1}) spectra of the L-LA oligomers. The γCH modes are predicted to appear in the 1245−1210 cm^{-1} range.

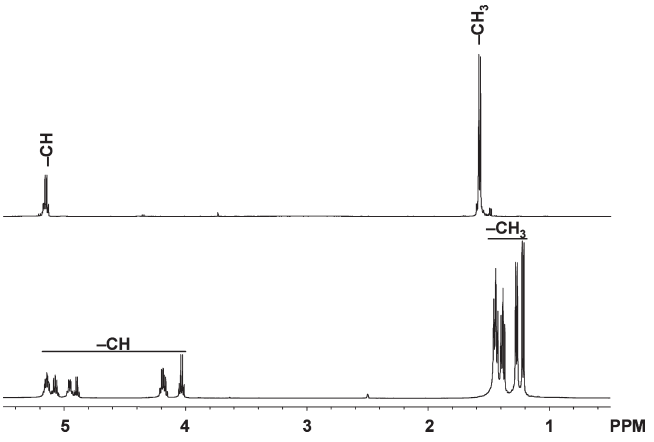

Figure 6. ^{1}H NMR spectra: top, PLLA homopolymer; bottom, mixture of L-LA oligomers.

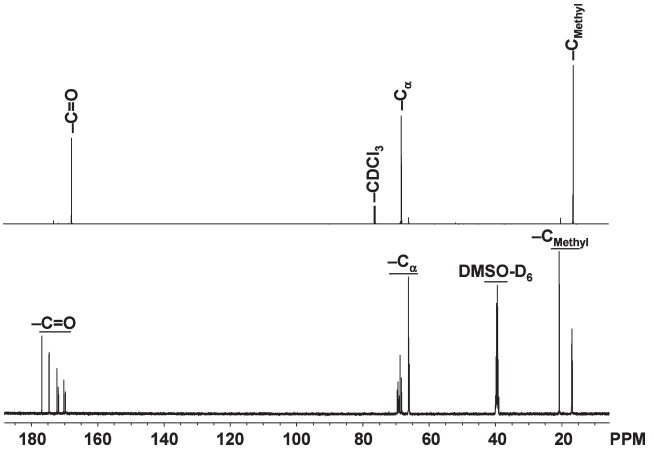

Figure 7. ^{13}C NMR spectra: top, PLLA homopolymer; bottom, mixture of L-LA oligomers.

The bands due to rocking modes of methyl groups (γCH_3) are predicted to appear in the 1135−1070 cm^{-1} range. Those revealed at ca. 1130 and ca. 1090 cm^{-1} in the experimental IR and Raman spectra of L-LA oligomers and PLLA homopolymer are then assigned to these modes. They appear as strong IR bands and medium intensity bands in the Raman spectrum.

The stretching vibration of the C−CH_3 groups ($\nu C_\alpha - C_\beta$) appears at ca. 1045 cm^{-1} in the spectra of L-LA oligomers and PLLA homopolymer.

The bands observed in the IR and Raman spectra of PLLA at ca. 960 and 920 cm^{-1} represent the amorphous and crystalline domains of the polymer, respectively.[32] Interestingly, the band at ca. 920 cm^{-1}, which reflects the crystalline phase of the polymer, has a correspondence in the vibrational spectra of the mixture of L-LA oligomers. However, the band at higher wavenumbers is absent in the vibrational spectra of that mixture. The band at ca. 920 cm^{-1} was previously attributed to the combination of the C−C backbone stretching ($\nu C_\alpha - C$) and the CH_3 rocking mode of PLLA crystals.[33] According to the theoretical predictions, the two bands, at ca. 960 and 920 cm^{-1}, are also assigned to the $\nu C_\alpha - C$ vibration. Finally, the bands due to the carbonyl rocking modes appear in the 755−740 cm^{-1} range.

NMR Spectra. Figures 6 and 7 depict the ^{1}H and ^{13}C NMR spectra of PLLA and of a mixture of small L-LA oligomers. Table 4 shows the calculated chemical shifts (^{1}H, ^{13}C, and ^{15}O) for the SS[SG′A]$_4$C conformation of L-LA pentamer and experimental chemical shifts (^{1}H and ^{13}C) with respect to TMS, used as standard, and DMSO-D_6, used as solvent, for the PLLA polymer. The reasonable agreement between the calculated chemical shifts for the L-LA pentamer and those observed for the PLLA homopolymer also validates the approximation here used, i.e., the use of a small system as pentamer as model to predict the conformational and spectroscopic properties of the homopolymer.

Tables 5 and 6 summarize the experimental results obtained for the small L-LA oligomers and for the PLLA homopolymer. The chemical shifts of the H_α protons of the homopolymer of L-LA were experimentally observed around 5 ppm. The calculated average chemical shift for the H_α protons in the conformer SS[SG′A]$_4$C of L-LA pentamer is 5.29 ppm, which agrees with the experimental value observed for the polymer. The protons of the methyl groups of the pentamer are predicted at ca. 1.56 ppm. These predictions are also in agreement with the experimental observations for PLLA, at ca. 1.47 ppm. In the ^{13}C NMR spectrum of the PLLA polymer, the signal due to the C(=O) moiety is observed at 170 ppm (and predicted at around 180 ppm). On the other hand, the C_α atoms in the pentamer are predicted to appear around 75 ppm and observed around 70 ppm. The C_{Methyl} signals appear at lower chemical shifts (calculated for the pentamer around 20 ppm). They were observed around 17 ppm in the experimental spectrum of the polymer.

The H_A and H_C positions in NMR spectra are intimately dependent on various factors, the water content being indeed extremely important, and the temperature and the sample concentration also playing an important role in the position of the protons. In order to investigate the influence of the environment (temperature variation and H_2O/D_2O content) on the exchange regime of the H_A and H_C protons of the mixture of L-LA oligomers in DMSO-D_6 solution, the following experiments (^{1}H NMR spectra) were recorded: (i) T_{room} (25 °C); 35 °C; 50 °C (for higher temperatures, exchange rates increase considerably, causing the NMR peaks to widen but fast exchange regime is not attained even at temperatures of 95 °C; see Figure S4); (ii) 1 and 3 μL of H_2O were added to the solution (see Figure S5); (iii) 3 μL of D_2O were added to the solution (see Figure S6). Adding a few drops of H_2O or D_2O to the solution gives rise to alterations in chemical exchange rates and resonances broaden even more significantly than due to temperature increase. In the presence of D_2O there is a considerable decrease in the resonance intensity of exchangeable protons due to substitution by deuterium.

It should be mentioned that the signal due to the H_C proton is much more sensitive to the temperature increase and water content in solution than that due to the H_A proton, which is clearly reflected in the great variation of the full width at half-maximum (fwhm) of the peak due to the former proton. This can be explained because the latter is involved in an intramolecular hydrogen bond (O−H_A...O=C) and is less acidic than the H_C, which make the H_A proton less accessible to H_2O/D_2O, as well as less sensitive to temperature rise.

Another point that should be mentioned is that due to the nature of the hydroxyl protons (considerable line width even in very dry samples due to exchange phenomena)

Table 4. Calculated GIAO [B3LYP/6-311++G(d,p)] Chemical Shifts (^{1}H, ^{13}C and ^{15}O) for the Conformation SS[SG′A]$_4$C of the L-LA Pentamer (Figure 3) and Experimental Chemical Shifts (^{1}H and ^{13}C) with Respect to TMS Used as Standard and DMSO-D_6 Used as Solvent, for the PLLA Polymer

	Δσ/ppm			Δσ/ppm	
atom[a]	calcd	exptl	atom[a]	calcd	exptl
$[H_\alpha]_A$	4.42	5.19	$[C_{Methyl}]_A$	22.51	16.50
$[H_\alpha]_{E1}$	5.63		$[C_{Methyl}]_{E1}$	20.38	
$[H_\alpha]_{E2}$	5.75		$[C_{Methyl}]_{E2}$	19.83	
$[H_\alpha]_{E3}$	5.51		$[C_{Methyl}]_{E3}$	19.71	
$[H_\alpha]_C$	5.13		$[C_{Methyl}]_C$	20.04	
average	5.29 (5.33)[c]		average	20.49 (20.54)	
$[H_{Methyl}]_A$[b]	1.52	1.47	$[C{=}O]_A$	185.17	169.53
$[H_{Methyl}]_{E1}$	1.57		$[C{=}O]_{E1}$	177.50	
$[H_{Methyl}]_{E2}$	1.56		$[C{=}O]_{E2}$	176.64	
$[H_{Methyl}]_{E3}$	1.55		$[C{=}O]_{E3}$	177.81	
$[H_{Methyl}]_C$	1.61		$[C{=}O]_C$	178.10	
average	1.56 (1.52)		average	179.04 (180.94)	
H_A	2.52	n.o.[d]	$[O_{Carboxyl}]_A$	215.41	n.i.[e]
H_C	5.73	n.o.	$[O_{Carboxyl}]_{E1}$	223.95	n.i.
$[C_\alpha]_A$	72.39	70.00	$[O_{Carboxyl}]_{E2}$	225.76	n.i.
$[C_\alpha]_{E1}$	75.80		$[O_{Carboxyl}]_{E3}$	228.51	n.i.
$[C_\alpha]_{E2}$	75.32		O_C	204.28	n.i.
$[C_\alpha]_{E3}$	75.91		$[O_{Carbonyl}]_A$	390.56	n.i.
$[C_\alpha]_C$	76.10		$[O_{Carbonyl}]_{E1}$	399.50	n.i.
average	75.10 (76.24)		$[O_{Carbonyl}]_{E2}$	400.61	n.i.
			$[O_{Carbonyl}]_{E3}$	401.68	n.i.
			$[O_{Carbonyl}]_C$	403.19	n.i.
			O_A	42.35	n.i.

[a] See Figure 3 for atom and monomeric units labeling. [b] Average over the three hydrogen atoms of the methyl group (−CH_3). [c] Results in parentheses arise from the calculations performed with aug-cc-pVTZ-J basis set. [d] n.o.: not observed. [e] n.i.: not investigated.

Table 5. Experimental ^{1}H NMR Chemical Shifts for the Monomer, Dimer, Trimer, Tetramer, and Homopolymer of L-LA[a]

	mon	dim		tri			tetra				penta[b]
C−H	4.03 (4.48)	4.18 (4.46)	4.92 (4.94)	4.20 (4.46)	5.10 (5.42)	4.98 (5.28)	4.20 (4.51)	5.10 (5.29)	5.17 (5.65)	4.98 (5.14)	5.19 (5.29)
$C-H_3$	1.22 (1.48)	1.28 (1.42)	1.39 (1.65)	1.28 (1.47)	1.45 (1.51)	1.41 (1.48)	1.28 (1.49)	1.45 (1.56)	1.47 (1.45)	1.41 (1.53)	1.47 (1.56)

[a] Values in parentheses are from GIAO [B3LYP/6-311++G(d,p)] calculated chemical shifts (average over all relevant conformers). [b] The experimental ^{1}H NMR chemical shifts for the homopolymer and pentamer are coincident.

it is not possible to distinguish between the peaks due to a particular oligomer (monomer, dimer, ..., pentamer) present in solution.

Table S17 shows the positions of the peaks due to H_C, H_A, and H_W (W means water) observed in experiments i, ii, and iii, presented in Figures S4−S6, as well as the fwhm of the peak due to the H_C protons.

NOESY experiment was recorded for the mixture of L-LA oligomers (see Figure S7). Concerning the preferred conformations adopted by the L-LA oligomers, the obtained information extracted from NOESY experiments was limited, with only two main pieces of information extracted from this experiment: (A) the H_A proton is close to the H_C proton and (B) the $H_{Methine}$ proton is close to the H_C proton.

It is important to stress here that, due to the lower resolution of the NOESY technique compared to unidimensional ^{1}H and ^{13}C NMR spectra, it is not possible using the first technique to distinguish between signals from different L-LA oligomers, contrarily to what succeeds in the later case.

From the full set of experiments and theoretical data one could conclude that interaction (A), as shown by the NOESY data, is due to only the monomer (see Figure 1)—which is indeed the predominant species in the studied sample. Indeed, the relative populations in the L-LA oligomers decrease from the monomer up to the pentamer, the latter being extremely low populated. On the other hand, interaction (B) revealed by the NOESY data can occur in all oligomers, being established between H_C and the adjacent methine proton [i.e., both interacting protons belong the acid unit (see Figure 3) and keep an approximately equal spatial arrangement in all oligomers].

dx.doi.org/10.1021/jp205033c |J. Phys. Chem. B 2012, 116, 9–21

Table 6. Experimental ^{13}C NMR Chemical Shifts for the Monomer, Dimer, Trimer, Tetramer, and Homopolymer of L-LA[a]

	mon	dim		tri		tetra		penta[b]	
C=O	176.30 (182.23)	174.09 (181.42)	171.70 (176.55)	174.01 (182.60)	171.25 (178.06)	169.74 (176.08)	171.18 (182.64)	169.69 (176.85)	169.31 (176.86)	169.25 (176.38)	169.53 (179.04)
C_α	65.76 (74.11)	65.62 (73.38)	68.27 (75.06)	65.62 (74.58)	67.88 (75.21)	68.98 (75.82)	65.52 (74.51)	67.80 (76.34)	68.61 (74.95)	69.14 (76.91)	70.00 (75.10)
C_{Methyl}	20.43 (24.23)	20.34 (24.47)	16.70 (19.00)	20.33 (22.61)	16.59 (18.93)	16.58 (19.61)	n.o. (23.05)	n.o. (19.59)	16.56 (19.15)	16.45 (19.32)	16.50 (20.49)

[a] Values in parentheses are from GIAO [B3LYP/6-311++G(d,p)] calculated chemical shifts (average over all relevant conformers). [b] The experimental ^{13}C NMR chemical shifts for the homopolymer and pentamer are coincident.

CONCLUSIONS

The conformations preferentially adopted by PLLA homopolymer chains were determined by a detailed investigation of the energetics and structural and spectroscopic characteristics of small L-LA oligomers (up to the pentamer). For that, the IR/Raman and $^1H/^{13}C$ NMR spectroscopies, known as being very sensitive techniques to structural aspects, were used together with B3LYP/6-311++G(d,p) calculations.

Information about the conformations of the PLLA chain, which has six independent types of dihedrals, $H-O_{Alcohol}-C-C$, $O_{Alcohol}-C-C=O$, $O=C-O_{Ester}-C$, $C-O_{Ester}-C-C$, $O_{Ester}-C-C=O$, and $O=C-O_{Acid}-H$, was gained step-by-step by considering the motifs of the subsequently larger L-LA oligomers. The preferred conformations adopted by the terminal $H-O_{Alcohol}-C-C$, $O_{Alcohol}-C-C=O$, and $O=C-O_{Acid}-H$ dihedrals were known from the monomer studies; i.e., they are *syn* (S), *syn* (S), *s-cis* (C), respectively. The conformations that the middle $O=C-O_{Ester}-C$, $C-O_{Ester}-C-C$, and $O_{Ester}-C-C=O$ dihedrals of the PLLA polymer preferentially adopt were known from the study of the dimer, trimer, and tetramer, being *syn* (S), *gauche*′ (G′), and *anti* (A), respectively. The preferential conformation adopted by the polymeric chain of PLLA homopolymer with n L-LA monomers was then determined as $SS[SG'A]_{n-1}C$.

The $O-H_A\cdots O=$ intramolecular H-bond was revealed to be the most relevant stabilizing interaction in L-LA oligomers. Other less important interactions can also stabilize the L-LA oligomers, such as $O-H_A\cdots O_C$, $O-H_A\cdots O_E$, $O-H_C\cdots O=$, $O-H_C\cdots O_A$, $O-H_C\cdots O_E$, $C-H_\alpha\cdots O=C_E$, and $C-H_{Methyl}\cdots O=C_E$.

The theoretical approach used in this work, i.e., the study of different oligomers of L-LA with increasing size, enabled the acquisition of information concerning the preferred conformations adopted by the chains of the PLLA polymer. Such approach saved much computational effort and simultaneously permitted to gather further details useful for the interpretation of the experimental data. Complex systems, such as polymers, can then be treated at higher levels of theory using quite small models. In this case, a small system as the L-LA pentamer was enough to simulate the structural and spectroscopic properties of PLLA homopolymer.

ASSOCIATED CONTENT

Supporting Information. GIAO DFT/B3LYP chemical shifts; IR spectra; B3LYP/6-311++G(d,p) conformers; H NMR spectra; NOESY spectra; structural and energetic parameters (Figures S1−S17; Tables S1−S17). This material is available free of charge via the Internet at http://pubs.acs.org.

AUTHOR INFORMATION

Corresponding Author
*E-mail sjarmelo@qui.uc.pt.

ACKNOWLEDGMENT

S.J. acknowledges "Fundação para a Ciência e Tecnologia", grant SFRH/BPD/22410/2005;

D.A.S.M. acknowledges "Fundação para a Ciência e Tecnologia", grant SFRH/BD/42245/2007; project PORTUGAL (FCT)/ARGENTINA (SECyT)—PO/07/006;

projects FCT-PTDC/QUI/71203/2006, and FCT-PTDC/QUI/119879/2009, also supported by COMPETE and FEDER.

REFERENCES

(1) Sodergard, A.; Stolt, M. *Prog. Polym. Sci.* **2002**, *27*, 1123.
(2) Sinclair, R. G. *J. Macromol. Sci., Pure Appl. Chem.* **1996**, *A33*, 585. Aou, K.; Hsu, S. L. *Macromolecules* **2006**, *39*, 3337.
(3) Jain, R. A. *Biomaterials* **2000**, *21*, 2475.
(4) Ikada, Y.; Tsuji, H. *Macromol. Rapid Commun.* **2000**, *21*, 117.
(5) Perego, G.; Cella, G. D.; Bastioli, C. *J. Appl. Polym. Sci.* **1996**, *59*, 37.
(6) De Santis, P.; Kovacs, A. J. *Biopolymers* **1968**, *6*, 299.
(7) Marques, D. A. S.; Jarmelo, S.; Baptista, C.; Gil, M. H. *Mod. Trends Polym. Sci. Epf 09* **2010**, *296*, 63.
(8) Espartero, J. L.; Rashkov, I.; Li, S. M.; Manolova, N.; Vert, M. *Macromolecules* **1996**, *29*, 3535.
(9) Chang, G.; Guida, W. C.; Still, W. C. *J. Am. Chem. Soc.* **1989**, *111*, 4379.
(10) Computational Chemistry, HyperChem Manual; Hypercube Inc.: Ontario, Canada, 1994.
(11) Becke, A. D. *Phys. Rev. A* **1988**, *38*, 3098. Lee, C. T.; Yang, W. T.; Parr, R. G. *Phys. Rev. B* **1988**, *37*, 785.
(12) McLean, A. D.; Chandler, G. S. *J. Chem. Phys.* **1980**, *72*, 5639.
(13) Schmidt, M. W.; Baldridge, K. K.; Boatz, J. A.; Elbert, S. T.; Gordon, M. S.; Jensen, J. H.; Koseki, S.; Matsunaga, N.; Nguyen, K. A.; Su, S. J.; Windus, T. L.; Dupuis, M.; Montgomery, J. A. *J. Comput. Chem.* **1993**, *14*, 1347.Gamess, 24 Mar 2007 (R1) ed.; Iowa State University, 2007
(14) Frisch, M. J.; Trucks, G. W.; Schlegel, H. B.; Scuseria, G. E.; Robb, M. A.; Cheeseman, J. R.; Montgomery, J. A.; Vreven, T.; Kudin, K. N.; Burant, J. C.; Millam, J. M.; Iyengar, S. S.; Tomasi, J.; Barone, V.; Mennucci, B.; Cossi, M.; Scalmani, G.; Rega, N.; Petersson, G. A.; Nakatsuji, H.; Hada, M.; Ehara, M.; Toyota, K.; Fukuda, R.; Hasegawa, J.; Ishida, M.; Nakajima, T.; Honda, Y.; Kitao, O.; Nakai, H.; Klene, M.; Li, X.; Knox, J. E.; Hratchian, H. P.; Cross, J. B.; Bakken, V.; Adamo, C.; Jaramillo, J.; Gomperts, R.; Stratmann, R. E.; Yazyev, O.; Austin, A. J.; Cammi, R.; Pomelli, C.; Ochterski, J. W.; Ayala, P. Y.; Morokuma, K.; Voth, G. A.; Salvador, P.; Dannenberg, J. J.; Zakrzewski, V. G.; Dapprich, S.; Daniels, A. D.; Strain, M. C.; Farkas, O.; Malick, D. K.; Rabuck, A. D.; Raghavachari, K.; Foresman, J. B.; Ortiz, J. V.; Cui, Q.; Baboul, A. G.; Clifford, S.; Cioslowski, J.; Stefanov, B. B.; Liu, G.; Liashenko, A.; Piskorz, P.; Komaromi, I.; Martin, R. L.; Fox, D. J.; Keith, T.; Al-Laham, M. A.; Peng, C. Y.; Nanayakkara, A.; Challacombe, M.; Gill, P. M. W.; Johnson, B.; Chen, W.; Wong, M. W.; Gonzalez, C.; Pople, J. A. *Gaussian 03*, revision D.01; Gaussian, Inc.: Wallingford, CT, 2004.
(15) Ditchfie., R. *Mol. Phys.* **1974**, *27*, 789.
(16) Jensen, F. *J. Chem. Theory Comput.* **2008**, *4*, 719.
(17) Peralta, J. E.; Scuseria, G. E.; Cheeseman, J. R.; Frisch, M. J. *Chem. Phys. Lett.* **2003**, *375*, 452. Provasi, P. F.; Aucar, G. A.; Sauer, S. P. A. *J. Chem. Phys.* **2001**, *115*, 1324.
(18) Kupka, T. *Magn. Reson. Chem.* **2009**, *47*, 674.
(19) Stewart, J. J. P. *J. Comput. Chem.* **1989**, *10*, 221.
(20) Stewart, J. J. P. *J. Mol. Model.* **2007**, *13*, 1173.
(21) Stewart, J. J. P. MOPAC2007, Computational Chemistry, Colorado Springs, CO, 2007.
(22) Reva, I. A.; Jarmelo, S.; Lapinski, L.; Fausto, R. *J. Phys. Chem. A* **2004**, *108*, 6982. Reva, I. D.; Jarmelo, S.; Lapinski, L.; Fausto, R. *Chem. Phys. Lett.* **2004**, *389*, 68.
(23) Jarmelo, S.; Fausto, R. *Phys. Chem. Chem. Phys.* **2002**, *4*, 1555.
(24) Borba, A.; Gómez-Zavaglia, A.; Lapinski, L.; Fausto, R. *Phys. Chem. Chem. Phys.* **2004**, *6*, 2101.
(25) Fausto, R. *J. Mol. Struct.* **1994**, *323*, 267.
(26) Scott, A. P.; Radom, L. *J. Phys. Chem.* **1996**, *100*, 16502. Fekete, Z. A.; Hoffmann, E. A.; Kortvelyesi, T.; Penke, B. *Mol. Phys.* **2007**, *105*, 2597.
(27) Curl, R. F. *J. Chem. Phys.* **1959**, *30*, 1529. O'Gorman, J. M.; Shand, W.; Schomaker, V. *J. Am. Chem. Soc.* **1950**, *72*, 4222. Riveros, J. M.; Wilson, E. B. *J. Chem. Phys.* **1967**, *46*, 4605. Miyazawa, T. *Bull. Chem. Soc. Jpn.* **1961**, *34*, 691.
(28) Teixeira Dias, J. J. C.; Fausto, R.; de Carvalho, L. *J. Mol. Struct.—Theochem* **1992**, *94*, 87. Fausto, R.; de Carvalho, L.; Teixeira Dias, J. J. C. *J. Comput. Chem.* **1992**, *13*, 799.
(29) Fausto, R.; Teixeira Dias, J. J. C. *J. Mol. Struct.—Theochem* **1987**, *35*, 381.
(30) Owen, N. L.; Sheppard, N. *Proc. Chem. Soc. London* **1963**, 264. Bailey, J.; North, A. M. *Trans. Faraday Soc.* **1968**, *64*, 1499. Piercy, J. E.; Subrahma, Sv. *J. Chem. Phys.* **1965**, *42*, 1475.
(31) Blazewicz, M.; Gajewska, M. C.; Paluszkiewicz, C. *J. Mol. Struct.* **1999**, *482*, 519.
(32) Vasanthan, N.; Ly, O. *Polym. Degrad. Stab.* **2009**, *94*, 1364.
(33) Zhang, J. M.; Tsuji, H.; Noda, I.; Ozaki, Y. *Macromolecules* **2004**, *37*, 6433.